deposition on CMC-544-treated cells also supports this advantage. Although, in this assay, some cases did not show an increase of compliment deposition, their viable cell counts had already decreased to 87–71% after the first 30 min of CDC assay. The cells that trapped more compliment deposition and were susceptible to CDC might have been damaged in the early phase of CDC assay. In this study, we could not show the combination efficacy of rituximab and CMC-544 on ADCC as CMC-544 might be quickly internalized after binding to CD22.

We showed here the rationale for the advantage of combined use of CMC-544 and rituximab in BCM. CMC-544 preserved the level of CD20 and decreased the level of CD55, both of which are closely related to resistance to rituximab.[6–8] Sequential combination of these agents, that is, CMC-544 followed by rituximab, may be a relevant way forward. Such combination approaches may enable more promising therapeutic approaches for the treatment of BCM especially in relapse or refractory to conventional treatments with rituximab.

Acknowledgements

We express our sincere gratitude to Wyeth Pharmaceuticals Inc. (USA) for their continuous support and for reviewing the article, and to Ms Yoshimi Suzuki, Ms Noriko Anma and Dr Kiyoshi Shibata (Equipment Center at Hamamatsu University School of Medicine) for technical assistance. This study was supported by Japanese grants-in-aid from the Ministry of Education, Culture, Sports, Science and Technology (19590552, 17590489).

References

1 Fisher RL, Shah P. Current trends in large cell lymphoma. *Leukemia* 2003; **17**: 1948–1960.
2 Fanale MA, Younes A. Monoclonal antibodies in the treatment of non-Hodgkin's lymphoma. *Drugs* 2007; **67**: 333–350.
3 Coiffier B. Rituximab therapy in malignant lymphoma. *Oncogene* 2007; **26**: 3603–3613.
4 Montserrat E, Moreno C, Esteve J, Urbano-Ispizua A, Giné E, Bosch F. How I treat refractory CLL. *Blood* 2006; **107**: 1276–1283.
5 Smith MR. Rituximab (monoclonal anti-CD20 antibody): mechanisms of action and resistance. *Oncogene* 2003; **22**: 7359–7368.
6 Bannerji R, Kitada S, Flinn IW, Pearson M, Young D, Reed JC *et al.* Apoptotic-regulatory and complement-protecting protein expression in chronic lymphocytic leukemia: relationship to *in vivo* rituximab resistance. *J Clin Oncol* 2003; **21**: 1466–1471.
7 Golay J, Lazzari M, Facchinetti V, Bernasconi S, Borleri G, Barbui T *et al.* CD20 levels determine the *in vitro* susceptibility to rituximab and complement of B-cell chronic lymphocytic leukemia: further regulation by CD55 and CD59. *Blood* 2001; **98**: 3383–3389.
8 Macor P, Tripodo C, Zorzet S, Piovan E, Bossi F, Marzari R *et al.* *In vivo* targeting of human neutralizing antibodies against CD55 and CD59 to lymphoma cells increases the antitumor activity of rituximab. *Cancer Res* 2007; **67**: 10556–10563.
9 Dahle J, Borrebaek J, Jonasdottir TJ, Hjelmerud AK, Melhus KB, Bruland ØS *et al.* Targeted cancer therapy with a novel low-dose rate alpha-emitting radioimmunoconjugate. *Blood* 2007; **110**: 2049–2056.
10 DiJoseph JF, Amelino DC, Boghhaert ER, Khandke K, Dougher MM, Sridharan L *et al.* Antibody-targeted chemotherapy with CMC544: a CD22-tageted immunoconjugate of calicheamicin for the treatment of B-lymphoid malignancies. *Blood* 2004; **103**: 1807–1814.
11 Zein N, Sinha AM, McGahren WJ, Ellestad GA. Calicheamicin gamma 1I: an antitumor antibiotic that cleaves double-stranded DNA site specifically. *Science* 1988; **240**: 1198–1201.
12 Fayad L, Patel H, Verhoef G, Cruczman M, Foran J, Gine E *et al.* Clinical activity of the immunoconjugate CMC-544 in B-cell malignancies: Preliminary report of the expanded maximum tolerated dose (MTD) cohort of a phase 1 study. *Blood* 2006; **108**: 766a, absr. #2711.
13 DiJoseph JF, Dougher MM, Kalyandrug LB, Armellino DC, Boghaert ER, Hamann PR *et al.* Antitumor efficacy of a combination of CMC-544 (inotuzumab ozogamicin), a CD22-targeted cytotoxic immunoconjugate of calicheamicin, and rituximab against non-Hodgkin's B-cell lymphoma. *Clin Cancer Res* 2006; **12**: 242–249.
14 Sugimoto Y, Sato S, Tsukahara S, Suzuki M, Okochi E, Gottesman MM *et al.* Coexpression of a multidrug resistance gene (MDR1) and herpes simplex virus thymidine kinase gene in a bicistronic retroviral vector Ha-MDR-IRES-TK allows selective killing of MDR1-transduced human tumors transplanted in nude mice. *Cancer Gene Ther* 1997; **4**: 51–58.
15 Matsui H, Takeshita A, Naito K, Shinjo K, Shigeno K, Maekawa M *et al.* Reduced effect of gemtuzumab ozogamicin (CMC-676) on P-glycoprotein and/or CD34-positive leukemia cells and its restoration by multidrug resistance modifiers. *Leukemia* 2002; **16**: 813–819.
16 Yasukawa M, Arai J, Kakimoto M, Sakai I, Kohno H, Fujita S. CD20-positive adult T-cell leukemia. *Am J Hematol* 2001; **66**: 39–41.
17 Toba K, Hanawa H, Fuse I, Sakaue M, Watanabe K, Uesugi Y *et al.* Difference in CD22 molecules in human B cells and basophils. *Exp Hematol* 2002; **30**: 205–211.
18 Hatanaka M, Seya T, Matsumoto M, Hara T, Nonaka T, Inoue N *et al.* Mechanisms by which the surface expression of the glycosylphosphatidylinositol- anchored complement regulatory proteins decayacceleratingfactor (CD55) and CD59 is lost in human leukaemia cell lines. *Biochem J* 1996; **314**: 969–976.
19 Naito K, Takeshita A, Shigeno K, Nakamura S, Fujisawa S, Shijo K *et al.* Caliceamicin-conjugated humanized anti-CD33 monoclonal antibody (gemtuzumab ozogamicin, CMC676) shows cytocydal effect on CD33-positive leukemia cell lines, but is inactive on P-glycoprotein-expressing sublines. *Leukemia* 2000; **14**: 1436–1443.
20 Takeshita A, Shinjo K, Naito K, Matsui H, Sahara N, Shigono K *et al.* Efficacy of gemtuzumab ozogamicin on ATRA- and arsenic-resistant acute promyelocytic leukemia (APL) cells. *Leukemia* 2005; **19**: 1306–1311.
21 Takei K, Yamazaki T, Sawada U, Ishizuka H, Aizawa S. Analysis of changes in CD20, CD55, and CD59 expression on established rituximab-resistant B-lymphoma cell lines. *Leuk Res* 2006; **30**: 625–631.
22 Karasawa S, Araki T, Yamamoto-Hino M, Miyawaki A. A green-emitting fluorescent protein from Galaxeidae coral and its monomeric version for use in fluorescent labeling. *J Biol Chem* 2003; **278**: 34167–34171.
23 Cheson BD. Monoclonal antibody therapy for B-cell malignancies. *Semin Oncol* 2006; **33**: S2–S14.
24 van der Kolk LE, Grillo-López AJ, Baars JW, van Oers MH. Treatment of relapsed B-cell non-Hodgkin's lymphoma with a combination of chimeric anti-CD20 monoclonal antibodies (rituximab) and G-CSF: final report on safety and efficacy. *Leukemia* 2003; **17**: 1658–1664.
25 Ziller F, Macor P, Bulla R, Sblattero D, Marzari R, Tedesco F. Controlling complement resistance in cancer by using human monoclonal antibodies that neutralize complement-regulatory proteins CD55 and CD59. *Eur J Immunol* 2005; **35**: 2175–2183.

Int J Hematol
DOI 10.1007/s12185-010-0492-1

ORIGINAL ARTICLE

The clinical characteristics of CD7$^+$ CD56$^+$ acute myeloid leukemias other than M0

Ritsuro Suzuki · Shigeki Ohtake · Jin Takeuchi · Masami Nagai · Yoshihisa Kodera · Motohiro Hamaguchi · Shuichi Miyawaki · Takahiro Karasuno · Shigetaka Shimodaira · Ryuzo Ohno · Shigeo Nakamura · Tomoki Naoe

Received: 2 June 2009 / Revised: 22 December 2009 / Accepted: 4 January 2010

Abstract Immunological phenotyping of acute leukemia have provided enormous and important information for the classification and lineage determination of leukemia. Forty-nine patients with CD7$^+$ CD56$^+$ acute myeloid leukemia (AML) were analyzed. There were 17 patients of M0, which corresponded to myeloid/NK cell precursor acute leukemia, and 32 patients of AML other than M0 (9 each for M1 and M2, one for M3, 3 for M4, 4 for M5 and 6 for M7). Age distribution was similar between these two groups, but CD7$^+$ CD56$^+$ M0 showed significant male predominance than CD7$^+$ CD56$^+$ M1–M7 (M:F = 15:2 vs. 15:17, $P = 0.006$). The disease localization and the hematological manifestations were different, showing fewer white blood cell counts and circulating leukemic blasts, less anemia, less thrombocytopenia and more frequent extramedullary involvement in M0 group. The prognosis was poor in both groups, and there was no statistical difference. These findings suggest that extramedullary involvement of myeloid/NK cell precursor acute

R. Suzuki (✉)
Department of HSCT Data Management,
Nagoya University School of Medicine,
1-1-20 Daiko-minami, Higashi-ku,
Nagoya 461-0047, Japan
e-mail: r-suzuki@med.nagoya-u.ac.jp

S. Ohtake
Third Department of Internal Medicine,
Kanazawa University School of Medicine,
Kanazawa, Japan

J. Takeuchi
Department of Internal Medicine,
Nihon University School of Medicine,
Tokyo, Japan

M. Nagai
First Department of Internal Medicine,
Kagawa Medical University, Takamatsu, Japan

Y. Kodera
Department of Internal Medicine,
Japanese Red Cross Nagoya First Hospital,
Nagoya, Japan

M. Hamaguchi
Department of Hematology,
National Hospital Organization,
Nagoya Medical Center, Nagoya, Japan

S. Miyawaki
Department of Internal Medicine,
Saiseikai Maebashi Hospital, Maebashi, Japan

T. Karasuno
Department of Internal Medicine,
Osaka Medical Center for Cancer
and Cardiovascular Diseases, Osaka, Japan

S. Shimodaira
Department of Internal Medicine,
Japanese Red Cross Nagano Hospital,
Nagano, Japan

R. Ohno
Aichi Cancer Center, Nagoya, Japan

S. Nakamura
Department of Pathology,
Nagoya University School of Medicine, Nagoya, Japan

T. Naoe
Department of Hematology and Oncology,
Nagoya University School of Medicine, Nagoya, Japan

Published online: 29 January 2010

leukemia is not directly derived from the presence of CD7 and CD56 antigens on leukemic cells. The poor prognosis of $CD7^+$ $CD56^+$ M1–M7 suggests that this phenotype may act as a prognostic factor for AML, but this should be confirmed in further studies.

Keywords Acute myeloid leukemia · Immunophenotyping · CD7 · CD56

1 Introduction

Acute myeloid leukemia (AML) comprises a heterogeneous group of diseases that differ in their etiology, pathogenesis, and prognosis. It was first classified by its morphology and cytochemical reactions in the French–American–British (FAB) classification [1] and the World Health Organization (WHO) classification [2]. In the past two decades, the immunological classification of AML has developed on the basis of progress on the use of monoclonal antibodies and flow-cytometric analyses [3–5]. Several phenotypic markers have been demonstrated to have clinical significance other than for diagnosis including detection of minimal residual disease [6, 7] and prognostication [8–10].

We previously identified an immunophenotypically novel AML with the $CD7^+$ $CD56^+$ myeloid $antigen^+$ phenotype and termed it "myeloid/natural killer (NK) cell precursor acute leukemia" [11]. Myeloid/NK cell precursor acute leukemia presents a similar phenotype to its normal counterpart (precursor NK cells with myeloid antigens) [12–14], but shows distinct clinicopathologic features [11, 15, 16]. Tumor cells of myeloid/NK cell precursor acute leukemia show immature blastic morphology and are positive for myeloid antigens, but are negative for the cytochemical myeloperoxidase (MPO) reaction, suggesting that this leukemia falls within the category of AML M0 according to the FAB classification. However, apart from its $CD7^+$ $CD56^+$ phenotype, its clinical presentation is quite different from those of other M0 leukemias [16]. Patients with myeloid/NK cell precursor acute leukemia frequently exhibit extramedullary involvement and lymphadenopathy with or without a mediastinal mass. Although they are responsive to AML-type chemotherapy, the prognosis is extremely poor, even for younger patients [11, 16]. In this context, it is necessary to understand whether the $CD7^+$ $CD56^+$ phenotype is responsible for these particular characteristics of myeloid/NK cell precursor acute leukemia. To clarify this issue, we collected data from patients with $CD7^+$ $CD56^+$ AML other than M0 (M1–M7), and compared their clinical characteristics with those of patients with myeloid/NK cell precursor acute leukemia [16].

2 Patients and methods

2.1 Patients

A total of 32 patients with $CD7^+$ $CD56^+$ AML other than M0 (M1–M7) were identified in the collaborating institutes of the Japan Adult Leukemia Study Group and the Japan Clinical Oncology Study Group. Data were collected with a survey form in participating institutions separately from prospective studies. The diagnosis of AML was based on the FAB and WHO classification [1, 17, 18]. Cases with extramedullary leukemia were included in this study, even though less than 20% of their bone marrow cells were leukemic [16]. The patients' records and clinical data were reviewed retrospectively. As for chemotherapeutic regimens, those containing high dose cytosine arabinoside (Ara-C) or those involving Ara-C for at least five consecutive days accompanied by anthracyclines for at least 3 days were categorized as AML-type chemotherapy. The clinical characteristics of patients with $CD7^+$ $CD56^+$ AML (M1–M7) were compared with those of patents with myeloid/NK cell precursor acute leukemia ($CD7^+$ $CD56^+$ AML M0) as previously described [16]. This study was approved by the Ethical Committee as a part of retrospective survey for NK cell-related tumors (approval #625-3).

2.2 Immunophenotyping

Flow-cytometric analyses were performed as previously described [11]. The reactivity for the following markers was analyzed: CD1, CD2, CD3, CD4, CD5, CD7, CD8, CD10, CD11b, CD13, CD14, CD15, CD16, CD19, CD20, CD25, CD33, CD34, CD38, CD41, CD56, CD57, CD71, CD117, CD122, HLA-DR, T cell receptor (TCR) $\alpha\beta$, TCR $\gamma\delta$, IgA, IgG, IgM, IgD, kappa, lambda, cytoplasmic CD3 (cyCD3), cyCD22, cyCD33, cyIgM, cyMPO, and terminal deoxynucleotidyl transferase (TdT). Cytoplasmic antigens and TdT were analyzed as previously described with fixation in 50% ethanol with 1% paraformaldehyde. Leukemic cells were judged as positive for each antigen when more than 20% of the gated cell reacted with the antibody.

2.3 Cytogenetic analysis

Leukemic cells were cultured, and the chromosomes were banded. Cytogenetic abnormalities were determined according to the International System for Human Cytogenetic Nomenclature [19].

2.4 Statistical analysis

The χ^2 test and Fisher's exact test were used to examine relationships between two factors, and the Mann–Whitney

U test was used to compare graded factors. Survival curves were estimated with the Kaplan–Meier method and compared by means of the log-rank test. Data were analyzed with STATA version 9 (College Station, TX) and Fisher (Nakayama-Shoten, Tokyo, Japan) statistical software.

3 Results

3.1 Patient characteristics

A total of 49 AML patients with the $CD7^+$ $CD56^+$ phenotype were identified in the collaborating institutes. Of these, 17 M0 patients had previously been reported as having myeloid/NK cell precursor acute leukemia. The clinical features of the 32 patients with $CD7^+$ $CD56^+$ AML (M1–M7) are listed in Table 1. The $CD7^+$ $CD56^+$ phenotype was recognized in all FAB subtypes except M6. Notably, 6 patients were found with AML M7. No recurrent structural abnormalities were identified by chromosome examinations. One patient showed t(15;17), but none presented with t(8;21), inv(16), or 11q23 translocations. Trisomy 4 was found in 3 patients. Total or partial deletions in chromosome 7 were seen in 4 patients. A comparison of the patients' characteristics with those of patients suffering from $CD7^+$ $CD56^+$ M0 is shown in Table 2. The median age of the patients was 49 years, and their age distribution was not statistically different from that of the $CD7^+$ $CD56^+$ AML

Table 1 Patient characteristics of the $CD7^+$ $CD56^+$ AML (M1–M7) group

No.	Age	Sex	FAB	WBC	Blast (%)	RBC	Plt	BM blast (%)	MPO (%)	Extra-medulla	LN	Others
1	21	M	M1	91,100	86.0	298	5.8	85.5	99.9	N	–	
2	21	M	M1	17,000	97.0	250	6.2	89.2	99.9	N	–	
3	36	M	M1	39,200	77.5	480	21.0	91.6	3.0	N	–	
4	45	F	M1	43,800	98.0	278	0.6	83.5	90.0	N	–	
5	47	M	M1	4,600	56.0	325	0.8	Dry tap	99.9	N	–	
6	50	M	M1	35,800	82.0	454	3.9	89.2	5.0	Y	+	
7	53	F	M1	149,300	94.0	377	2.8	85.0	90.0	N	–	
8	54	M	M1	203,600	93.0	240	3.5	86.6	28.0	N	–	
9	70	M	M1	3,000	0	369	23.8	4.0	11.0[a]	Y	+	Spleen
10	26	F	M2	2,800	0	348	13.0	0.4	95.0[a]	Y	+	Tonsil
11	29	F	M2	31,400	75.4	439	2.0	61.9	99.2	N	–	
12	32	F	M2	1,700	0	309	23.7	55.7	61.5	N	–	
13	49	F	M2	10,100	13.0	369	1.6	53.6	50.0	N	–	
14	63	F	M2	3,600	54.0	367	3.9	48.8	100.0	N	–	
15	63	M	M2	13,200	93.5	359	1.7	87.9	90.0	Y	+	
16	70	M	M2	22,200	90.0	170	0.6	49.0	98.0	Y	–	Skin
17	74	F	M2	3,600	54.0	203	2.1	85.2	96.0	N	–	
18	76	F	M2	1,800	13.0	109	2.2	43.2	41.0	Y	–	Spleen
19	37	F	M3	4,300	90.0	213	0.4	50.0	80.0	N	–	
20	34	F	M4	3,000	14.0	104	1.7	87.6	99.0	N	–	
21	59	M	M4	55,290	39.0	246	5.7	67.4	81.5	Y	–	Skin
22	86	F	M4	211,900	60.0	264	4.2	79.0	80.0	N	–	
23	21	F	M5a	269,700	96.0	248	5.7	98.8	90.0	Y	+	Gingiva
24	23	F	M5a	540,000	98.0	210	4.4	99.0	10.0	Y	–	Meningeal
25	53	M	M5a	13,320	79.0	376	7.0	89.0	80.0	N	–	
26	17	M	M5b	3,900	20.0	409	18.8	83.5	0	N	–	
27	31	M	M7	600	20.0	344	22.2	83.0	0	N	–	
28	42	M	M7	2,100	24.0	239	11.6	81.5	18.0	N	–	
29	48	F	M7	17,000	92.0	215	37.8	70.5	2.0	N	–	
30	68	F	M7	2,800	69.0	350	2.6	54.0	10.0	N	–	
31	70	M	M7	2,600	1.5	229	9.9	20.0	0	N	–	
32	74	F	M7	3,600	32.0	400	6.0	32.4	0	N	–	

[a] Examined at the time of recurrence/progression

Table 2 Comparison of $CD7^+$ $CD56^+$ AML patient characteristics (M0 versus M1–M7)

	$CD7^+$ $CD56^+$ AML M1–M7 ($n = 32$)	$CD7^+$ $CD56^+$ AML M0 ($n = 17$)	*P* value
Age (years), median (range)	49 (17–86)	46 (15–81)	0.32
Sex (male/female)	15/17	15/2	0.002
Peripheral blood count			
WBC (/μl), median (range)	11,650 (600–540,000)	4,500 (1000–51,000)	0.04
PB blast (%), median (range)	64.5 (0–98.0)	5.0 (0–95.0)	0.0006
Hb (g/dl), median (range)	9.7 (4.1–14.2)	13.1 (5.5–17.0)	0.004
PLT ($\times 10^4$/μl), median (range)	4.3 (0.4–37.8)	12.8 (3.9–38.5)	0.002
Sites of involvement			
Bone marrow			
Median blast (%)	81.5%	80.0%	0.59
No marrow involvement	2	5	0.04
Extramedullary	9 (28%)	14 (82%)	0.0004
Lymph node	5	12	0.0002
Mediastinum	1	4	0.04
Liver and/or spleen	2	2	0.43
Skin	2	1	0.73
Others	3	3	0.34

WBC white blood cell, *PB* peripheral blood, *PLT* platelets

M0 patients. There was almost an equal sex distribution for $CD7^+$ $CD56^+$ M1–M7 (male:female = 15:17), and the male:female ratio was significantly different from that of $CD7^+$ $CD56^+$ M0 ($P = 0.006$). The peripheral blood cell count at diagnosis showed a significantly higher white blood cell count ($P = 0.04$) and higher leukemic cell percentage ($P = 0.0006$) in the $CD7^+$ $CD56^+$ M1–M7 patients than in the $CD7^+$ $CD56^+$ M0 patients. In addition, the red blood cell and platelet counts for the former were significantly lower than those for the latter (Table 2). Overall, the $CD7^+$ $CD56^+$ M1–M7 patients showed many peripheral blood count abnormalities, which is comparable to standard AML.

Two $CD7^+$ $CD56^+$ M1–M7 patients did not show bone marrow (BM) involvement at the initial diagnosis, but the other cases showed a high percentage of BM leukemic cells. However, both of the 2 cases without BM involvement at the initial presentation progressed predominantly in the BM with manifestations of acute leukemia. Extramedullary involvement was recognized in 9 patients of the $CD7^+$ $CD56^+$ M1–M7 group (28%), which was significantly lower than the number in the $CD7^+$ $CD56^+$ M0 group ($P = 0.0004$). Although lymph node involvement was the most common manifestation of the extramedullary diseases of the $CD7^+$ $CD56^+$ M1–M7 group, the absolute incidence was significantly lower than that in the $CD7^+$ $CD56^+$ M0 group ($P = 0.0002$), as was the incidence of mediastinal involvement ($P = 0.04$).

In summary, no clinical manifestations of "myeloid/NK cell precursor acute leukemia" were recognized in the $CD7^+$ $CD56^+$ M1–M7 group.

3.2 Immunophenotyping

The immunophenotypic characteristics of the patients are summarized in Table 3. By definition, all patients were positive for both CD7 and CD56 antigens. Most of the cases were positive for CD13, CD33, CD34, CD117, and HLA-DR, while all were negative for lymphoid-specific markers including CD16 and CD57. CD41 was expressed in all 6 cases of megakaryoblastic leukemia (AML M7). Several lymphoid markers that are known to be also expressed in AML, such as CD2, CD4, CD5, CD10, and TdT were expressed in some of the patients. The incidence was higher in the M1 and M7 cases.

3.3 Therapeutic response and prognosis

In the $CD7^+$ $CD56^+$ AML M1–M7 group, 20 of the 29 patients that were initially treated with AML-type chemotherapy attained complete remission (CR), whereas none of the two cases treated with CHOP chemotherapy did (Table 4). Because of the low numbers of patients, the difference was not statistically significant. Another patient could not receive any chemotherapy due to their poor condition. The CR rate was 67% (6 of 9) for M1, 56% (5 of 9) for M2, 100% (1 of 1) for M3, 67% (2 of 3) for M4, 75% (3 of 4) for M5, and 50% (3 of 6) for M7. Of the 20 patients who achieved CR, two received allogeneic hematopoietic stem cell transplantation in first CR, and both are alive without disease. Eight of the 20 patients experienced disease recurrence.

Table 3 Phenotypic characteristics of CD7+ CD56+ AML patients (M1–M7)

FAB	M1 ($n = 9$)	M2 ($n = 9$)	M3 ($n = 1$)	M4 ($n = 3$)	M5 ($n = 4$)	M7 ($n = 6$)	Total ($n = 32$)	%
CD1	0/3	0/2	ND	0/2	0/1	0/3	0/12	0
CD2	0/8	0/9	1/1	0/3	0/3	1/6	2/30	7
CD3	0/9	0/8	0/1	0/3	0/4	0/6	0/31	0
CD4	0/9	0/5	0/1	0/3	0/3	2/6	2/27	7
CD5	2/9	0/7	0/1	0/3	0/4	1/6	3/30	10
CD7	9/9	9/9	1/1	3/3	4/4	6/6	32/32	100
CD8	0/9	0/5	0/1	0/3	0/3	0/5	0/26	0
CD10	2/9	0/8	1/1	0/3	0/4	1/6	4/31	13
CD11b	1/7	0/2	1/1	1/2	1/2	4/4	8/18	44
CD13	7/9	9/9	1/1	2/3	4/4	3/6	26/32	81
CD14	0/9	0/8	1/1	1/3	0/4	1/6	3/31	10
CD15	1/5	1/3	0/1	1/2	1/2	0/4	4/17	24
CD16	0/1	0/4	ND	0/1	ND	0/5	0/11	0
CD19	0/9	0/9	0/1	0/3	0/4	0/6	0/32	0
CD20	0/9	0/9	0/1	0/3	0/4	0/6	0/32	0
CD25	0/6	0/2	0/1	0/2	0/3	0/4	0/18	0
CD33	8/9	9/9	1/1	3/3	4/4	6/6	31/32	97
CD34	9/9	7/7	1/1	2/3	4/4	4/6	27/30	90
CD41	0/7	0/4	0/1	0/3	0/2	6/6	6/17	35
CD56	9/9	9/9	1/1	3/3	4/4	6/6	32/32	100
CD57	0/3	0/2	ND	ND	ND	0/3	0/8	0
CD117	2/2	1/1	ND	ND	1/1	1/2	5/6	83
HLA-DR	7/9	8/8	1/1	2/3	4/4	4/6	26/31	84
TdT	1/3	ND	ND	ND	ND	0/2	1/5	20

ND not determined

Table 4 Therapy and response

	CD7+ CD56+ AML (M1–M7)	CD7+ CD56+ AML M0
CR rate		
AML chemotherapy	20/29 (68%)	7/9 (78%)
NHL chemotherapy	0/2[a] (0%)	0/5 (0%)
P value	0.12	0.02

CR complete remission, *AML* acute myeloid leukemia, *NHL* non-Hodgkin's lymphoma

[a] Both patients presented with extramedullary myeloid leukemia

The overall survival (OS) and disease-free survival (DFS) curves are shown in Fig. 1a. The prognosis of the CD7+ CD56+ M1–M7 patients was also poor, and no statistical difference was found from that of the CD7+ CD56+ M0 (myeloid/NK cell precursor acute leukemia) group.

4 Discussion

In this study, we demonstrated that CD7+ CD56+ AML M1–M7 does not show extramedullary leukemic involvement, which is a typical manifestation of myeloid/NK cell precursor acute leukemia, but does have a poor prognosis. The reason for the peculiar clinical manifestation of myeloid/NK cell precursor acute leukemia remains unclear, but our current results suggest that it is not caused by the expression of two key molecules, CD7 and CD56.

The low incidence of extramedullary involvement in our CD7+ CD56+ AML M1–M7 cases is consistent with the findings of previous large-scale studies that investigated CD56 expression in AML [20, 21]. We could not identify any specific features for the CD7+ CD56+ AML M1–M7 group except for a preference for FAB M7 (6 of 32 cases). The association of CD56 expression and megakaryoblastic leukemia has been documented in a study with a small number of the cases [22], but was not examined in a recent, larger study [23]. Although several similarities exist between AML M0 and M7, such as male predominance, negativity for the cytochemical MPO reaction, myeloid antigen expression, and poor prognosis [23], other clinical characteristics were different between the AML M0 and M7 CD7+ CD56+ phenotypes. This is particularly important for the correct diagnosis of myeloid/NK cell precursor acute leukemia. In the CD7+ CD56+ M1–M7 group, we

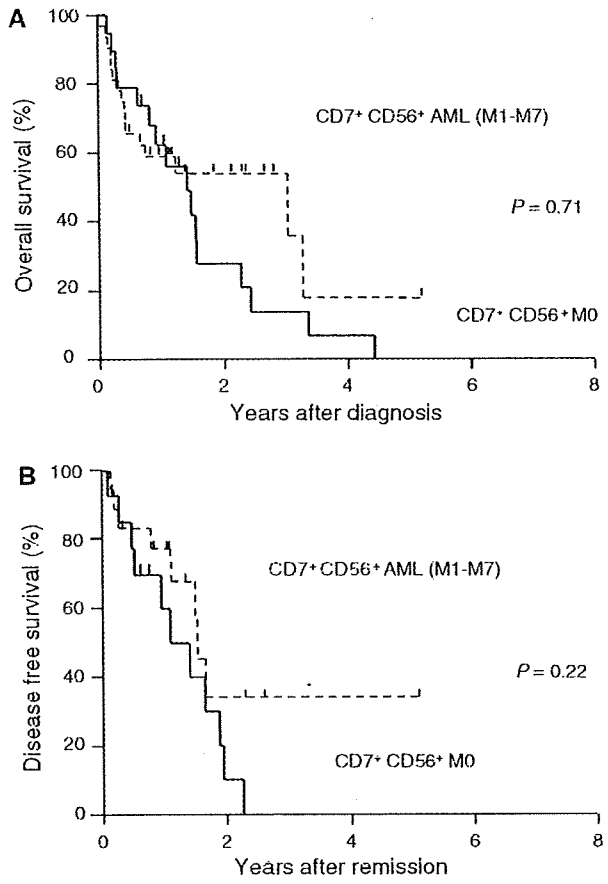

Fig. 1 Overall survival (a) and disease-free survival (b) curves of $CD7^+$ $CD56^+$ AML patients. *Thick lines* indicate survival curves of $CD7^+$ $CD56^+$ M0 and *broken lines* indicate those of $CD7^+$ $CD56^+$ AML M1–M7. No statistical differences were found between the two groups

identified one case with AML M3. This case showed the t(15;17) karyotype and responded to therapy with all-*trans* retinoic acid, indicating that the patient did not have myeloid/NK cell acute leukemia [24, 25] but typical M3.

The reason for the difference in extramedullary involvement between myeloid/NK cell precursor acute leukemia and $CD7^+$ $CD56^+$ AML M1–M7 remains unclear. Because CD56 was expressed in every case by definition, the extramedullary tumorigenesis does not directly derive from the hemophilic adhesion by CD56. Other adhesion molecules or chemokine/chemokine receptor might be responsible for this difference, which needs further investigations. Another hypothesis is that differentiation status of these leukemias is different. Since the origin of myeloid/NK cell precursor acute leukemia has been speculated as myeloid antigen-positive T/NK bi-potential progenitor [12, 13], the leukemic cell may retain affinity to lymph node or mediastinum.

The appropriate therapeutic approach for $CD7^+$ $CD56^+$ M1–M7 patients remains unknown. Expression of CD56 has been documented in various types of AML [20, 21], including specific subtypes, i.e., AML M2 with t(8;21) [26], AML M3 [27–29]. It is currently accepted as a marker of poor prognosis in AML [30–32]. Furthermore, the prognosis for NK cell malignancies, which are generally positive for CD56, is mostly poor [33–35], as is that for anaplastic large cell lymphoma [36], but not for those of peripheral T cell lymphoma, unspecified [37] or diffuse large B cell lymphoma. In this context, CD56 does not seem to cause the poor prognosis, but is rather a surrogate marker of poor prognosis. Hematopoietic stem cell transplantation, which was performed in several of our cases, is a treatment option [38], but this approach needs to be examined further in prospective studies. New agents such as CD56 monoclonal antibody conjugated with toxin or radio isotope are also good candidates [39, 40].

In summary, we found that $CD7^+$ $CD56^+$ M1–M7 shows a low incidence of extramedullary involvement, which is different from $CD7^+$ $CD56^+$ M0 or myeloid/NK cell precursor acute leukemia, but it still has a poor prognosis.

Acknowledgments This work was supported in part by a Grant-in-Aid for the Second-Term Comprehensive 10-year Strategy for Cancer Control from the Ministry of Health, Labour, and Welfare; a Grant-in-Aid for Science on Primary Areas (Cancer Research); and a Grant-in-Aid for Encouragement of Young Scientists from the Ministry of Education, Science, and Culture, Japan.

Appendix

The authors thank the collaborators from the following institutions for providing the patients' data and specimens: Akita University School of Medicine; Ohta Nishinouchi Hospital; Jikei University School of Medicine; University of Tokyo; Toranomon Hospital; Tokyo Metropolitan Komagome Hospital; Tokyo Medical University; Yaizu Municipal Hospital; Aichi Cancer Center; Nagoya City University School of Medicine; Social Insurance Kyoto Hospital; Nara Medical University; Kansai Medical University; Hyogo College of Medicine; Kochi University School of Medicine; Nagasaki University School of Medicine; Oita Prefectural Hospital.

References

1. Bennett JM, Catovsky D, Daniel M-T, et al. Proposals for the classification of the acute leukaemias. French–American–British (FAB) co-operative group. Br J Haematol. 1976;33:451–8.
2. Jaffe ES, Harris NL, Stein H, Vardiman JW. World Health Organization classification of tumours. Pathology & genetics:

tumours of haematopoietic and lymphoid tissues. Lyon: IARC Press; 2001.
3. Bene MC, Castoldi G, Knapp W, et al. Proposals for the immunological classification of acute leukemias. Leukemia. 1995; 9:1783–6.
4. Jennings CD, Foon KA. Recent advances in flow cytometry: application to the diagnosis of hematologic malignancy. Blood. 1997;90:2863–92.
5. Haferlach T, Kern W, Schnittger S, Schoch C. Modern diagnostics in acute leukemias. Crit Rev Oncol Hematol. 2005; 56:223–34.
6. Syrjala M, Anttila VJ, Ruutu T, Jansson SE. Flow cytometric detection of residual disease in acute leukemia by assaying blasts co-expressing myeloid and lymphatic antigens. Leukemia. 1994;8:1564–70.
7. San Miguel JF, Martinez A, Macedo A, et al. Immunophenotyping investigation of minimal residual disease is a useful approach for predicting relapse in acute myeloid leukemia patients. Blood. 1997;90:2465–70.
8. Bradstock K, Matthews J, Benson E, Page F, Bishop J. Prognostic value of immunophenotyping in acute myeloid leukemia. Australian Leukaemia Study Group. Blood. 1994;84:1220–5.
9. Legrand O, Perrot JY, Baudard M, et al. The immunophenotype of 177 adults with acute myeloid leukemia: proposal of a prognostic score. Blood. 2000;96:870–7.
10. Chang H, Salma F, Yi QL, Patterson B, Brien B, Minden MD. Prognostic relevance of immunophenotyping in 379 patients with acute myeloid leukemia. Leuk Res. 2004;28:43–8.
11. Suzuki R, Yamamoto K, Seto M, et al. CD7$^+$ and CD56$^+$ myeloid/natural killer cell precursor acute leukemia: a distinct hematolymphoid disease entity. Blood. 1997;90:2417–28.
12. Sanchez MJ, Muench MO, Roncarolo MG, Lanier LL, Phillips JH. Identification of a common T/natural killer cell progenitor in human fetal thymus. J Exp Med. 1994;180:569–76.
13. Shibuya A, Nagayoshi K, Nakamura K, Nakauchi H. Lymphokine requirement for the generation of natural killer cells from CD34+ hematopoietic progenitor cells. Blood. 1995;85:3538–46.
14. Perez SA, Sotiropoulou PA, Gkika DG, et al. A novel myeloid-like NK cell progenitor in human umbilical cord blood. Blood. 2003;101:3444–50.
15. Suzuki R, Nakamura S. Malignancies of natural killer (NK) cell precursor: myeloid/NK cell precursor acute leukemia and blastic NK cell lymphoma/leukemia. Leuk Res. 1999;23:615–24.
16. Suzuki R, Murata M, Kami M, et al. Prognostic significance of CD7$^+$ CD56$^+$ phenotype and chromosome 5 abnormalities for acute myeloid leukemia M0. Int J Hematol. 2003;77:482–9.
17. Bennett JM, Catovsky D, Daniel M-T, et al. Proposal for the recognition of minimally differentiated acute myeloid leukemia (AML-M0). Br J Haematol. 1991;78:325–9.
18. Jaffe ES, Harris NL, Stein H, et al. Tumours of haematopoietic and lymphoid tissues. Lyon: IARC Press; 2001.
19. ISCN 2005: an International system for Human Cytogenetic Nomenclature. In: Shaffer LG, Tommerup N, editors. Basal: Karger; 2005.
20. Seymour JF, Pierce SA, Kantarjian HM, Keating MI, Estey EH. Investigation of karyotypic, morphologic and clinical features in patients with acute myeloid leukemia blast cells expressing the neural cell adhesion molecule (CD56). Leukemia. 1994;8:823–6.
21. Thomas X, Vila L, Campos L, Sabido O, Archimbaud E. Expression N-CAM (CD56) on acute leukemia cells: relationship with disease characteristics and outcome. Leuk Lymphoma. 1995;19:295–300.
22. Ikushima S, Yoshihara T, Matsumura T, et al. Expression of CD56/NCAM on hematopoietic malignant cells. A useful marker for acute monocytic and megakaryocytic leukemias. Int J Hematol. 1991;54:395–403.
23. Tallman MS, Neuberg D, Bennett JM, et al. Acute megakaryocytic leukemia: the Eastern Cooperative Oncology Group experience. Blood. 2000;96:2405–11.
24. Scott AA, Head DR, Kopecky KJ, et al. HLA-DR−, CD33+, CD56+ CD16− myeloid/natural killer cell acute leukemia: a previously unrecognized form of acute leukemia potentially misdiagnosed as French–American–British acute myeloid leukemia-M3. Blood. 1994;84:244–55.
25. Girodon F, Carli P-M, Favre B, et al. Acute myeloid leukemia with hypergranular cytoplasm: a differential diagnosis of acute promyelocytic leukemia. Leuk Res. 2000;24:979–82.
26. Baer MR, Stewart CC, Lawrence D, et al. Expression of the neural cell adhesion molecule CD56 is associated with short remission duration and survival in acute myeloid leukemia with t(8;21)(q22;q22). Blood. 1997;90:1643–8.
27. Murray CK, Estey E, Paietta E, et al. CD56 expression in acute promyelocytic leukemia: a possible indicator of poor treatment outcome? J Clin Oncol. 1999;17:293–7.
28. Ferrara F, Morabito F, Martino B, et al. CD56 expression is an indicator of poor clinical outcome in patients with acute promyelocytic leukemia treated with simultaneous all-*trans*-retinoic acid and chemotherapy. J Clin Oncol. 2000;18:1295–300.
29. Ito S, Ishida Y, Oyake T, et al. Clinical and biological significance of CD56 antigen expression in acute promyelocytic leukemia. Leuk Lymphoma. 2004;45:1783–9.
30. Raspadori D, Damiani D, Lenoci M, et al. CD56 antigenic expression in acute myeloid leukemia identifies patients with poor clinical prognosis. Leukemia. 2001;15:1161–4.
31. Di Bona E, Sartori R, Zambello R, Guercini N, Madeo D, Rodeghiero F. Prognostic significance of CD56 antigen expression in acute myeloid leukemia. Haematologica. 2002;87:250–6.
32. Raspadori D, Damiani D, Michieli M, et al. CD56 and PGP expression in acute myeloid leukemia: impact on clinical outcome. Haematologica. 2002;87:1135–40.
33. Suzuki R. Leukemia and lymphoma of natural killer cells. J Clin Exp Hematopathol. 2005;45:51–70.
34. Oshimi K. Progress in understanding and managing natural killer-cell malignancies. Br J Haematol. 2007;139:532–44.
35. Suzuki R, Takeuchi K, Ohshima K, Nakamura S. Extranodal NK/T-cell lymphoma: diagnosis and treatment cues. Hematol Oncol. 2008;26:66–72.
36. Suzuki R, Kagami Y, Takeuchi K, et al. Prognostic significance of CD56 expression for ALK-positive and ALK-negative anaplastic large cell lymphoma of T/null cell phenotype. Blood. 2000;96:2993–3000.
37. Asano N, Suzuki R, Kagami Y, et al. Clinicopathologic and prognostic significance of cytotoxic molecule expression in nodal peripheral T-cell lymphoma, unspecified. Am J Surg Pathol. 2005;29:1284–93.
38. Suzuki R, Suzumiya J, Nakamura S, et al. Hematopoietic stem cell transplantation for natural killer-cell lineage neoplasms. Bone Marrow Transplant. 2006;37:425–31.
39. Tassone P, Gozzini A, Goldmacher V, et al. In vitro and in vivo activity of the maytansinoid immunoconjugate huN901–N2′-deacetyl-N2′-(3-mercapto-1-oxopropyl)-maytansine against CD56+ multiple myeloma cells. Cancer Res. 2004;64:4629–36.
40. Ishitsuka K, Jimi S, Goldmacher VS, et al. Targeting CD56 by the maytansinoid immunoconjugate IMGN901 (huN901-DM1): a potential therapeutic modality implication against natural killer/T cell malignancy. Br J Haematol. 2008;141:129–31.

European Journal of Haematology 84 (229–238)

ORIGINAL ARTICLE

BCR-ABL-independent and RAS/MAPK pathway-dependent form of imatinib resistance in Ph-positive acute lymphoblastic leukemia cell line with activation of EphB4

Momoko Suzuki[1,2], Akihiro Abe[1], Shizuka Imagama[3], Yuka Nomura[1], Ryohei Tanizaki[1], Yosuke Minami[1], Fumihiko Hayakawa[1], Yoshie Ito[4], Akira Katsumi[1], Kazuhito Yamamoto[5], Nobuhiko Emi[6], Hitoshi Kiyoi[7], Tomoki Naoe[1]

[1]Department of Hematology and Oncology, Nagoya University Graduate School of Medicine, Nagoya; [2]Department of Hematology, Komaki Municipal Hospital, Komaki, Aichi; [3]Department of Hematology, Nagoya Medical Center, Nagoya; [4]Yokkaichi City Public Health Center, Yokkaichi, Mie; [5]Department of Hematology, Aichi Cancer Center, Nagoya; [6]Department of Hematology, Fujita Health University, Toyoake, Aichi; [7]Department of Infectious Disease, Nagoya University Graduate School of Medicine, Nagoya, Japan

Abstract

Objective: We investigated the mechanism responsible for imatinib (IM) resistance in Philadelphia chromosome-positive acute lymphoblastic leukemia (Ph^+ ALL) cell lines. *Methods:* We established cell lines from a patient with Ph^+ ALL at the time of first diagnosis and relapsed phase and designated as NPhA1 and NPhA2, respectively. We also derived IM-resistant cells, NPhA2/STIR, from NPhA2 under gradually increasing IM concentrations. *Results:* NPhA1 was sensitive to IM (IC_{50} 0.05 μm) and NPhA2 showed mild IM resistance (IC_{50} 0.3 μm). NPhA2/STIR could be maintained in the presence of 10 μm IM. Phosphorylation of MEK and ERK was slightly elevated in NPhA2 and significantly elevated in NPhA2/STIR compared to NPhA1 cells. After treatment with IM, phosphorylation of MEK and ERK was not suppressed but rather increased in NPhA2 and NPhA2/STIR. Active RAS was also increased markedly in NPhA2/STIR after IM treatment. The expression of BCL-2 was increased in NPhA2 compared to NPhA1, but no further increase in NPhA2/STIR. Proliferation of NPhA2/STIR was significantly inhibited by a combination of MEK inhibitor and IM. Analysis of tyrosine phosphorylation status with a protein tyrosine kinase array showed increased phosphorylation of EphB4 in NPhA2/STIR after IM treatment. Although transcription of EphB4 was suppressed in NPhA1 and NPhA2 after IM treatment, it was not suppressed and its ligand, ephrinB2, was increased in NPhA2/STIR. Suppression of EphB4 transcripts by introducing short hairpin RNA into NPhA2/STIR partially restored their sensitivity to IM. *Conclusions:* These results suggest a new mechanism of IM resistance mediated by the activation of RAS/MAPK pathway and EphB4.

Key words Philadelphia chromosome-positive acute lymphoblastic leukemia; BCR-ABL; imatinib resistance; RAS/MAPK pathway; EphB4

Correspondence Akihiro Abe, MD, Department of Hematology and Oncology, Nagoya University Graduate School of Medicine, 65 Tsurumaicho, Showaku, Nagoya 466-8550, Japan. Tel: +81 52 744 2145; Fax: +81 52 744 2161; e-mail: aakihiro@med.nagoya-u.ac.jp

Accepted for publication 26 November 2009

doi:10.1111/j.1600-0609.2009.01387.x

The treatment of BCR-ABL-positive leukemia changed dramatically after the development of imatinib (IM). It has become a first-line agent in chronic phase chronic myelogenous leukemia (CML), and the 5-yr survival rate has improved greatly, together with a decrease in the rate of transformation to blastic crisis (1, 2). Acute lymphoblastic leukemia with Philadelphia chromosome (Ph^+ ALL) also arises from BCR-ABL positive progenitors, and use of IM in combination with conventional chemotherapy helps in extending the survival time (3). However, the effect of IM as a single agent for Ph^+ ALL is limited, and therefore relapse and resistance are continuing problems (4, 5).

Most prevalent mechanisms of IM resistance are point mutations in the kinase domain of ABL that preclude

the binding of IM (6, 7) and kinase inhibitors that overcome the effects of ABL kinase domain mutations have been developed (8). Many other mechanisms have also been reported to contribute to IM resistance; these include *BCR-ABL* gene amplification, BCR-ABL protein overexpression (9, 10), decreased intracellular IM concentration (11, 12), activation of other protein tyrosine kinases (PTKs) (13), and overexpression of BCL-2 (14). It has been reported that malignant hematopoietic progenitor cells from patients with CML are insensitive to IM and that CML stem cells remain in $CD34^+CD38^-$ fractions in bone marrow (BM) even after successful IM therapy (15, 16). Therefore, a strategy for overcoming BCR-ABL-independent IM resistance is an important requirement.

Although the mechanism of IM resistance in CML has been intensively investigated, fewer studies have examined IM resistance in Ph^+ ALL (17). Here, we investigated the mechanism of non-specifically induced mild resistance and IM-induced strong resistance in Ph^+ ALL cell lines.

Materials and methods

Patient and cell culture

The patient was a 64-yr-old woman who was diagnosed with Ph^+ ALL in 2002. She received chemotherapy and achieved remission, but relapsed 2 yr later. The karyotype was 46,XX,t(9;22)(q34;q11) at first diagnosis and relapsed phase. She had never been treated with IM. Heparinized BM samples were obtained with informed consent at initial diagnosis and during the relapse phase. Mononuclear cells were separated by Ficoll–Conray gradient centrifugation. The cells were cultivated in RPMI 1640 medium (Sigma, St. Louis, MO, USA) containing 20% fetal bovine serum (FBS) (Gibco-BRL, Grand Island, NY, USA), 100 IU/mL penicillin G (Meiji Seika, Tokyo, Japan), and 100 μg/mL streptomycin (Meiji Seika) and maintained in RPMI 1640 with 10% FBS. Cultures were performed at 37°C in a 5% CO_2-humidified atmosphere in an incubator. K562 cells were maintained in RPMI 1640 with 10% FBS.

Cell proliferation assay and reagents

To investigate the effect of kinase inhibitors on NPhA1, NPhA2, and NPhA2/STIR cells (2×10^4 per well) were added to 96-well plates in 100 μL RPMI containing 10% FBS with varying concentrations of IM, PI3-K inhibitor LY294002 (Promega, Madison, WI, USA), MEK inhibitor U0126 (Promega), SRC kinase inhibitor PP2 (Calbiochem, San Diego, CA, USA), or JAK2 inhibitor AG490 (Calbiochem). IM (Gleevec, STI-571) was provided by Novartis Pharmaceuticals (Basel, Switzerland). Tetra-Color One cell proliferation assay (Seikagaku Co., Tokyo, Japan) was performed as described previously (18). Briefly, the plates were incubated at 37°C for 72–96 h before the addition of a mixture of tetrazolium [2-(2-methoxy-4-nitrophenyl)-3-(4-nitrophenyl)-5-(2,4-disulfophenyl)-2H-tetrazolium, monosodium salt] and an electron carrier (1-methoxy-5-methylphenazium methylsulfate) (final volume 110 μL per well). The cells were incubated for an additional hour at 37°C, and absorption at 450 nm was measured using an ELISA plate reader.

Antibodies

The antibodies used were as follows: anti-phospho-AKT antiserum (Cell Signaling Technology, Beverly, MA, USA), rabbit anti-AKT antiserum (Cell Signaling Technology), rabbit anti-phospho-p44/42 MAPK antiserum (Cell Signaling Technology), rabbit anti-p44/42 MAPK antiserum (Cell Signaling Technology), rabbit anti-phospho-MEK 1/2 antiserum (Cell Signaling Technology), rabbit anti-MEK 1/2 antiserum (Cell Signaling Technology), rabbit anti-STAT3 antiserum (Santa Cruz Biotechnology, Santa Cruz, CA, USA), rabbit anti-phospho-STAT5 antiserum (Cell Signaling Technology), rabbit anti-STAT5A antiserum (R&D Systems, Minneapolis, MN, USA), rabbit anti-phospho-JAK2 antiserum (Upstate Biotechnology, Temecula, CA, USA), rabbit anti-JAK2 antiserum (Upstate Biotechnology), anti-phosphotyrosine mAb 4G10 (Millipore, Billerica, MA, USA), anti-EphB4 antiserum (R&D Systems), BCL2 (Cell Signaling Technology), $BCL\text{-}X_L$ (Cell Signaling Technology), HRP-linked whole anti-mouse IgG antibody (GE Healthcare Bio-Sciences, Tokyo, Japan), and HRP-linked whole anti-mouse and anti-rabbit IgG antibody (GE Healthcare Bio-Sciences).

Flow cytometry

Cell surface antigens were determined by staining with a combination of phycoerythrin (PE)-conjugated antibodies and FITC-conjugated antibody, and analyzed by FACSCalibur (Becton Dickinson, Franklin Lakes, NJ, USA) according to the manufacturer's instructions. Samples were mixed and incubated with an appropriate volume of antibodies for 30 min on ice. The PE-conjugated antibodies used were anti-human CD13, CD33, CD56 antibodies (BD Biosciences, San Jose, CA, USA); anti-human CD2, CD5, CD7, and CD8 antibodies (Beckman Coulter, San Jose, CA, USA); and anti-CD10 antibody (Dako Cytomation, Fort Collins, CO, USA). The FITC-conjugated antibodies used were anti-human HLA-DR antibody (BD Biosciences), and anti-CD3, CD4, CD19, CD34, and CD41 antibodies (Beckman Coulter). An additional

reaction with FITC and PE-labeled isotype control antibodies (BD Biosciences) was performed as a negative control. A PE-conjugated monoclonal antibody of a murine anti-human Pgp (BD Biosciences) was used to determine the expression of the *MDR1* gene product. Analyses were performed using CELLQUEST software (BD). For DNA histograms, cells were washed with phosphate-buffered saline (PBS) and re-suspended in PBS containing 0.2% Triton X-100 and 50 g/mL propidium iodide (Sigma). Then, the DNA histograms were quantified by flow cytometry as described previously (19).

Western blotting

Cells were washed in PBS at 4°C and solubilized in a lysis buffer: 10 mM Tris–HCl (pH 7.8), 150 mM NaCl, 1% NP-40, 1 mM EDTA, CompleteMini™ protease inhibitor cocktail (Roche, Mannheim, Germany), and phosphatase inhibitor cocktail 1 and 2 (Sigma). The cell lysates were centrifuged, and the supernatants were corrected. For immunoblotting, cell lysates were boiled with electrophoresis SDS sample buffer for 3 min, separated by SDS/PAGE, and transferred onto polyvinylidine difluoride (PVDF) membranes (Bio-Rad, Hercules, CA, USA). The membrane blots were blocked with 5% skim milk in Tris–buffered saline (TBS) containing 0.1% Tween 20 (TBS-T) or with blocking buffer (15 mmol/L NaCl; 10 mmol/M malic acid; and 1% blocking reagent, pH 7.5, for the detection of 4G10) for 1 h at 37°C followed by incubation with primary antibodies in TBS-T for 2 h at room temperature. Following washing, the membranes were incubated with HRP-linked whole anti-mouse IgG antibody (GE Healthcare Bio-Sciences) in TBS-T for 2 h at room temperature. After washing, an enhanced chemiluminescence assay was performed and positive bands were detected on X-ray films.

RAS activation assay

pGEX-Raf-Ras binding domain (RBD) was a generous gift from Drs. Michinari Hamaguchi and Takashi Senga, Nagoya University. GST-Raf-RBD was purified and RAS activation was measured as described previously (20). In brief, the cells were treated with or without 10 μM IM for 4 h and then lysed with lysis buffer containing 25 mM Tris–HCl (pH 7.2), 150 mM NaCl, 1% NP-40, 1 mM dithiothreitol, 5 mM $MgCl_2$, 5% glycerol, 1 mM phenylmethylsulfonyl fluoride, and 10 μg/mL of aprotinin and 10 μg/mL of leupeptin at 4°C. The cell lysates were then centrifuged and supernatants were transferred to chilled Eppendorf tubes containing 20 μg of GST-Raf-RBD immobilized beads, and incubated for 1 h at 4°C. Small amounts (20 μL) of lysates were used as the loading control. The samples were washed four times with 1 mL lysis buffer, and eluted with 2× SDS loading buffer with 2% 2-mercaptoethanol. The samples were separated by 13% SDS-PAGE and transferred to PVDF membrane and then the immunoprecipitates were probed with anti-RAS antibody (Upstate Biotechnology).

Phosphorylation of tyrosine kinase protein array

Expression of phosphorylated PTKs was detected using the Phosphorylation Antibody Array kit (RayBiotech, Norcross, GA, USA). NPhA1, NPhA2, NPhA2/STIR, and IM-treated cells of these lines were washed and solubilized in cold cell lysis buffer. Samples were centrifuged, and supernatants were collected. One hundred micrograms of each sample was incubated with PTK array membranes spotted with various anti-PTK antibodies. Procedures were according to the manufacturer's protocol. Array signals were visualized by chemiluminescence detection using X-ray film. Densitometric quantifications of spot intensity were performed using an LAS-4000 mini image analyzer (Fujifilm, Tokyo, Japan).

Detection of EphB4 and ephrinB2 mRNA by reverse transcription (RT)-PCR

Total RNA was extracted from each cell line using RNA STAT-60™ (Tel-Test, Inc. Friendswood, TX, USA). First-strand cDNA was reverse-transcribed using oligo(dT) primers and moloney murine leukemia virus reverse transcriptase. PCR amplification was performed with TaKaRa Taq™ (Takara, Otsu, Japan) for 26 or 30 cycles using oligonucleotide primers (95°C for 30 s, 60°C for 30 s, 72°C for 1 min). The *EphB4* primers used were EphB4-1554F (5′-CGGCCAGGAACATCACAGCCAGAC-3′) and EphB4-1848R (5′-CACCTGCACCAATCACCTCTTCAATC-3′). The *ephrinB2* primers are ephrinB2-288F (5′-CCCTCTCCTCAACTGTGCCAAACC-3′) and ephrinB2-727R (5′-CAGCAAGAGGACCACCAGCGTGAT-3′). PCR reaction products were electrophoresed on 1.5% agarose gels and stained with ethidium bromide. Densitometric quantification of band intensity was analyzed as described earlier.

Induction of short hairpin (sh)RNA

Oligonucleotides for shRNA were designed and provided from iGENE Therapeutics (Tokyo, Japan). The oligonucleotides for EphB4-sh1 were sense (5′-GATCCGGGCAAATACGGATAGTATACGTGTGCTGTCCGTATACTGTCCGTGTTTGTCCTTTTTAT-3′) and antisense (5′-CGATAAAAAGGACAAACACGGACAGTATACGGACAGCACACGTATACTATCCGTATTTGCCCG-3′).

The oligonucleotides for EphB4-sh2 were sense (5′-GATCCGAGGGGACTTGTTTCGCTAACGTGTGCTGTCCGTTAGTGAAACAGGTTCCCTCTTTTTAT-3′) and antisense (5′-CGATAAAAAGAGGGAACCTGTTTCACTAACGGACAGCACACGTTAGCGAAACAAGTCCCCTCG-3′).

To construct shRNA-expressing retrovirus vectors, each set of primers was annealed and inserted between *Bam*HI and *Cla*I sites of the pSINsi-hU6 retroviral vector (Takara). Control vector carrying scramble oligonucleotide (pSINsi-hU6-SO) was purchased from Takara. To generate pseudotype viruses, we co-transfected 10 μg of pSINsi-hU6-SO, pSINsi-hU6/EphB4-sh1 or pSINsi-hU6/EphB4-sh2 with 10 μg pCGCGP using calcium phosphate co-precipitation, as reported previously (21). Culture medium was replaced with 8 mL fresh medium 8 h after transfection, and pseudotype virus was collected 48 h after transfection. To establish NPhA2/STIR/sh1 and NPhA2/STIR/sh2 cells, NPhA2/STIR cells were infected with 4 mL of each virus supernatant in the presence of 5 μg/mL protamine. After 48 h, the shRNA-expressing cells were selected with 1 mg/mL G418 (Sigma) in RPMI medium, and at 3 wk, the surviving cells were analyzed.

Results

Establishment of Ph$^+$ ALL cell lines and IM-resistant cell line

Continuously growing cells were obtained from BM samples at first diagnosis and in the relapse phase and were named NPhA1 and NPhA2, respectively; doubling times were 36 and 30 h, respectively. We cultured NPhA1 and NPhA2 cells with increasing concentrations of IM to generate IM-resistant sublines. The concentration of IM was initially 1 nM and increased gradually to 10 μM. Highly IM-resistant cells, named NPhA2/STIR cells, were obtained from NPhA2 after 6 months and maintained in the presence of 10 μM IM. Under this condition, the doubling time of the NPhA2/STIR line was about 36 h. IM-resistant cells could not be established from NPhA1. NPhA1 and NPhA2 were maintained over 1 yr and NPhA2/STIR was maintained over 6 months in the presence of 10 μM of IM before starting this study. These cell lines carry minor BCR-ABL and showed similar surface antigen expression: CD2$^-$, CD3$^-$, CD4$^-$, CD5$^-$, CD8$^-$, CD10$^+$, CD13^{low}, CD19$^+$, CD33$^-$, CD34$^-$, CD41$^-$, CD56$^-$. The karyotypes of NPhA1, NPhA2 and NPhA2/STIR in the metaphase cells were 45,XX, der(8;12)(q10;q10),t(9;22)(q34;q11)(6/6), 46,XX,t(9;22)(q34;q11)(18/18), and 46,XX, add(2)(q33),t(9;22)(q34;q11)(20/20), respectively. NPhA1 with additional chromosomal abnormality was clonally selected from the primitive leukemia cells at first diagnosis, but NPhA2 has the same abnormality with the primitive leukemia cells at relapse phase. NPhA2/STIR obtained additional chromosomal abnormality of add(2)(q33) to NPhA2, which may relate with IM resistance.

Characterization of IM resistance in NPhA2 and NPhA2/STIR cells

Tetra Color One cell proliferation assays were performed on cells exposed to 0.01, 0.03, 0.1, 0.3, 1, 3, or 10 μM IM

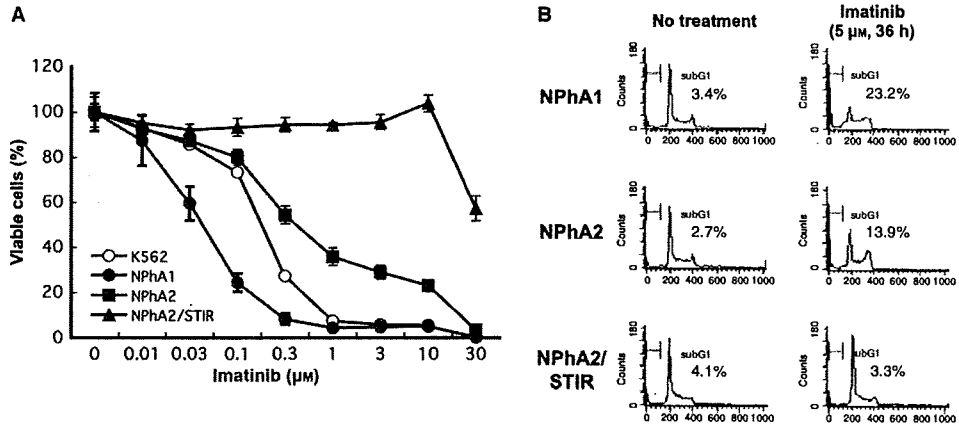

Figure 1 Characterization of imatinib (IM) sensitivity of NPhA1, NPhA2, and NPhA2/STIR cells. (A) IM sensitivity of cell lines derived from a Philadelphia chromosome-positive acute lymphoblastic leukemia patient. Each cell line was incubated with IM at the indicated concentration for 96 h. The cell proliferation assay was performed in triplicate, and mean absorption values with standard deviations are represented. Three repeat experiments showed similar results. (B) Cell cycle analysis by propidium iodide staining after treatment with IM. Each cell line was cultured in the presence or absence of 5 μM IM for 36 h. The cell cycle and cell death were evaluated by FACS analysis.

(Fig. 1A). On day 4, we evaluated the concentration of IM necessary to induce a 50% decrease in the number of viable cells as measured by the OD index. The IC_{50} was 0.05 μM for NPhA1, 0.3 μM for NPhA2, and 30 μM for NPhA2/STIR. NPhA2 cells acquired non-specifically induced IM resistance after a series of conventional chemotherapy without IM. NPhA1 cells were more sensitive but NPhA2 cells were more resistant to IM than K562 cells. Moreover, the concentration of IM needed for 50% reduction in the number of viable cells after 4 d of exposure to IM was about 100 times higher in the resistant NPhA2/STIR line compared to that in NPhA2 cells. Lines NPhA1 and NPhA2 did not show cell cycle-specific arrest, but the subG1 fraction increased after treatment with IM (Fig. 1B). IM did not affect the cell cycle distribution in NPhA2/STIR cells. Surface expression of MDR1 was not detected in NPhA2 and NPhA2/STIR cells by FACS analysis. No mutation was detected by direct sequencing with RT-PCR in kinase domain of the *BCR-ABL* gene (data not shown).

Phosphorylation of molecules involved in cell proliferation after IM treatment

We examined the phosphorylation of molecules that are involved in cell proliferation after IM treatment (Fig. 2A). Each cell was treated with IM for 6 h, and cell lysates were subjected to western blot analysis. The phosphorylation of BCR-ABL was decreased in NPhA2 cells, and phosphorylation of STAT5 paralleled with that of phospho-BCR-ABL after IM treatment. The phosphorylation level of MEK, ERK, and STAT3 was higher in NPhA2 compared with NPhA1 cells and was higher in NPhA2/STIR cells than in NPhA2 and NPhA1 cells. In particular, although phosphorylation of ABL was completely absent in all cells and phosphorylation of STAT5 was also suppressed, phosphorylation of MEK and ERK was increased in NPhA2, and especially in NPhA2/STIR cells, when treated with 10 μM IM for 6 h. Phosphorylation of AKT did not show any difference after IM treatment. We also examined expression of BCL-2 and BCL-X_L, and found that BCL-2 was increased but BCL-X_L was not altered in NPhA2 and NPhA2/STIR cells.

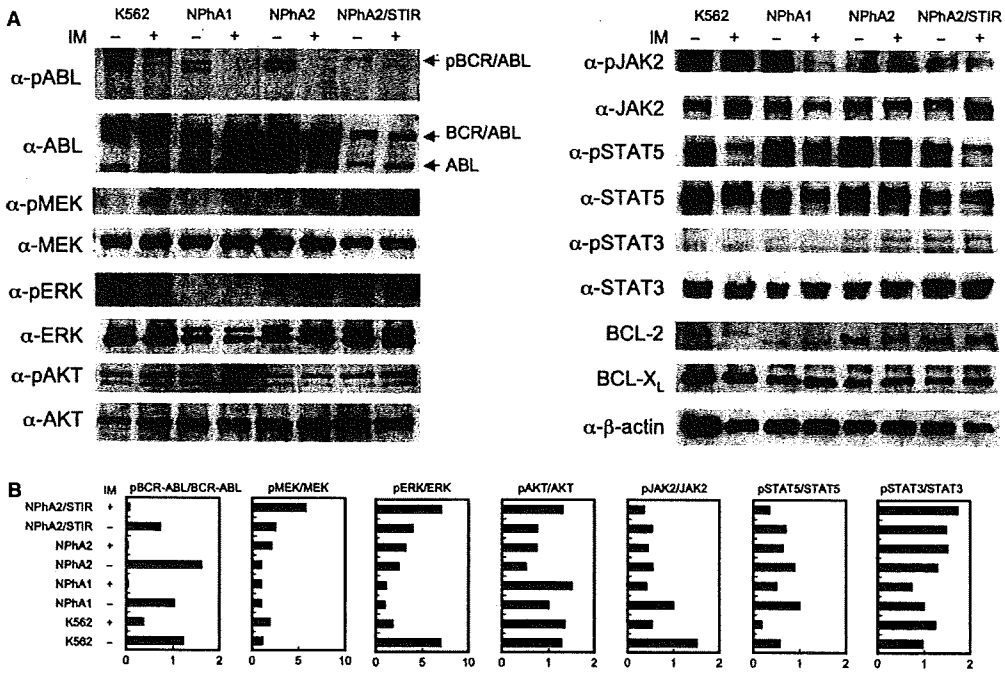

Figure 2 Phosphorylation and expression of molecules involved in cell proliferation and survival after imatinib (IM) treatment. (A) Phosphorylation and expression of signal molecules were analyzed by western blotting. Each cell line was treated or not treated with 10 μM IM for 6 h. Phosphorylation of ABL, MEK, ERK, AKT, JAK2, STAT5, and STAT3 was detected by phosphospecific antibodies. Expression of BCL-2 and BCL-X_L proteins is also shown. The experiments were repeated three times and showed similar results. (B) For quantification of band intensities, western blots were scanned with a high-resolution scanner, and the density of bands was quantified using ImageJ software (NIH, Bethesda, MD, USA). The data were shown as phosphorylated to total protein ratio that was calculated as relative value to the data of NPhA1 without IM as 1.

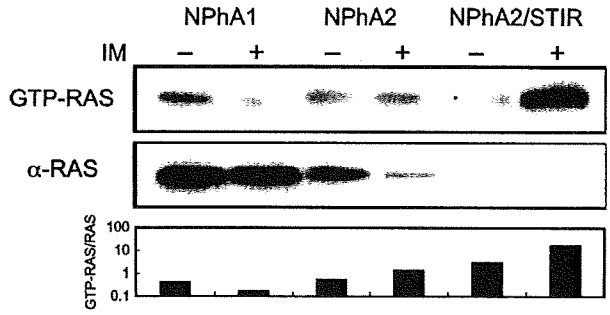

Figure 3 RAS activation assay. Each cell line was treated or not treated with 10 μM imatinib for 4 h and then the RAS assay was performed. Band intensities were determined as described before and shown as the value of GTP-RAS to total RAS ratio.

MEK/ERK is a downstream signaling protein of the RAS pathway. Therefore, we next examined RAS activity after IM treatment. We found that RAS was activated in NPhA1, NPhA2, and NPhA2/STIR cells, and that active RAS was decreased in NPhA1, but significantly increased in NPhA2/STIR cells after 4 h of exposure to 10 μM IM, although the basic level of expression of RAS protein was decreased in NPhA2/STIR cells (Fig. 3). These results indicate that the enhanced activation of MEK–MAPK pathway by IM in NPhA2/STIR cells occurred downstream of RAS activation.

Sensitivity to kinase inhibitors

We analyzed the sensitivity of NPhA1, NPhA2, and NPhA2/STIR cells to the kinase inhibitors MEK inhibitor (U0126), PI3K inhibitor (LY249002), SRC family kinase inhibitor (PP2), and JAK2 inhibitor (AG490). As shown in Fig. 4A, U0126 partially inhibited cell proliferation, especially in NPhA2/STIR cells. LY249002 and AG490 partially inhibited proliferation, but there was no specificity for IM-resistant cells. PP2 did not have any significant effects.

Combined treatment with the MEK inhibitor and IM had a synergistic effect on the suppression of NPhA2 proliferation, but synergism was not observed when the PI3K inhibitor was combined with IM (Fig. 4B).

Analysis of phosphorylation of PTKs

Phosphorylation of PTKs may contribute to IM resistance. To explore this possibility, the phosphorylation level of PTKs was determined using the Phosphorylation

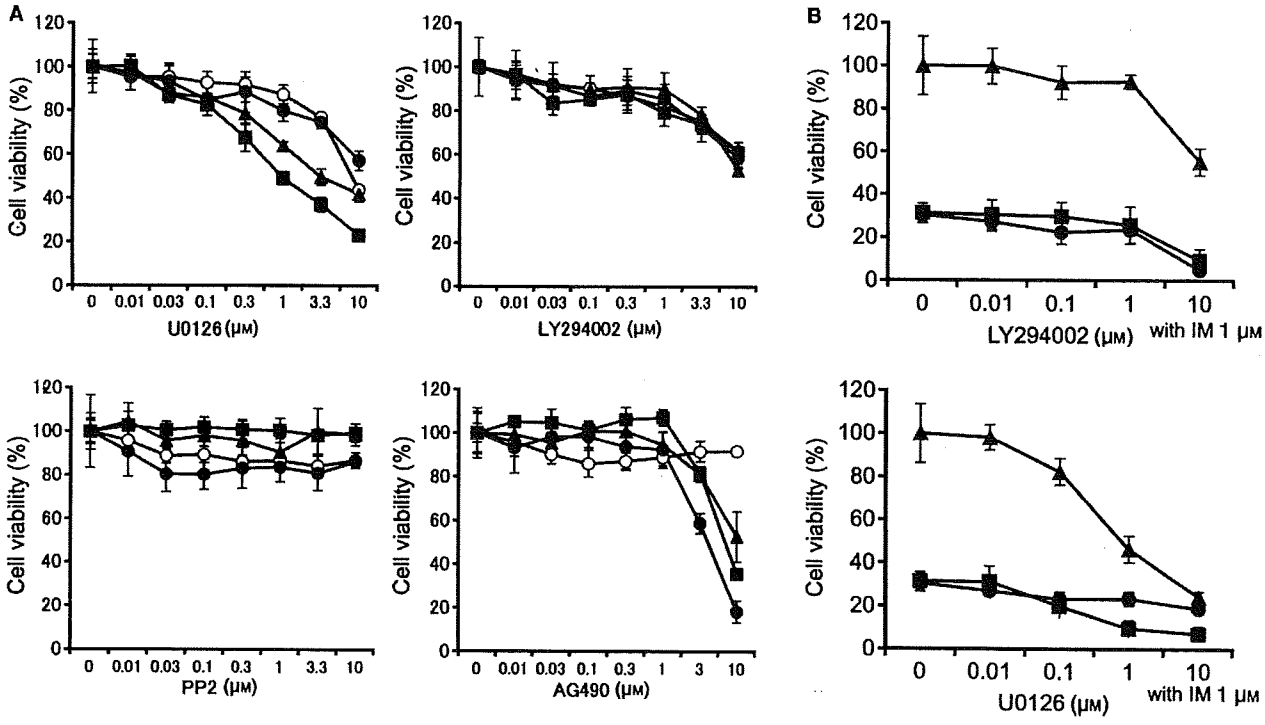

Figure 4 Sensitivity to kinase inhibitors and their combination. (A) Effect of MEK inhibitor (U0126), PI3K inhibitor (LY249002), SRC family kinase inhibitor (PP2), and JAK2 inhibitor (AG490) in K562 (○), NPhA1 (●), NPhA2 (■), and NPhA2/STIR (▲) cells was examined with the Tetra Color One assay. (B) Combined effect of imatinib (IM) with LY249002 or U0126. NPhA1 (●), NPhA2 (■), and NPhA2/STIR (▲) cells were incubated with 1 μM IM and LY249002 or U0126 at the indicated concentration for 96 h. The cell proliferation assay was performed in triplicate, and mean absorption values with standard deviations are represented.

Antibody Array kit with cell lysates of NPhA1, NPhA2, and NPhA2/STIR cells and corresponding IM-treated cells. This phospho-PTK array can simultaneously profile 71 different known human phosphorylated PTKs. The assay conserves time and samples because a large number of PTKs can be evaluated simultaneously using the same quantity of sample. Phosphorylation status was analyzed by densitometric quantification, and data for representative PTKs are shown in Fig. 5. The quality of the array was confirmed by the phosphorylation level of BCR-ABL, which was suppressed after the IM treatment and was consistent with the data of western blotting (Fig. 2). Phosphorylation of many Src family kinases, LYN, HCK and FGR, was suppressed after treatment with IM, and this suppression was paralleled by phosphorylation of BCR-ABL (Fig. 5). Phosphorylation of JAK2 was also inhibited by IM in three NPhA cell lines (Figs 2 and 5). Note that phosphorylation of EphB4 was increased in NPhA2/STIR cells after treatment with IM, but decreased in NPhA1 and NPhA2 cells. We therefore analyzed the role of EphB4 in the IM resistance of NPhA2/STIR cells.

Expression of EphB4 and ephrinB2 and phosphorylation of EphB4 in each cell line

We analyzed the mRNA expression of *EphB4* and *ephrinB2* in NPhA1, NPhA2, and NPhA2/STIR cells before and after treatment with IM (Fig. 6A). The expression of *EphB4* was inhibited in NPhA1 and NPhA2, but was not changed in NPhA2/STIR cells after treatment with IM. The expression of *ephrinB2* was increased in NPhA2 cells, which showed mild IM resistance, but the *EphB4* was inhibited after IM treatment. NPhA2/STIR cells showed higher expression of *EphB4* and *ephrinB2* than NPhA1 cells, with no decrease even after IM treatment. The phosphorylation of EphB4 was inhibited in NPhA1and NPhA2 cells but increased in NPhA2/STIR cells after treatment with IM (Fig. 6B).

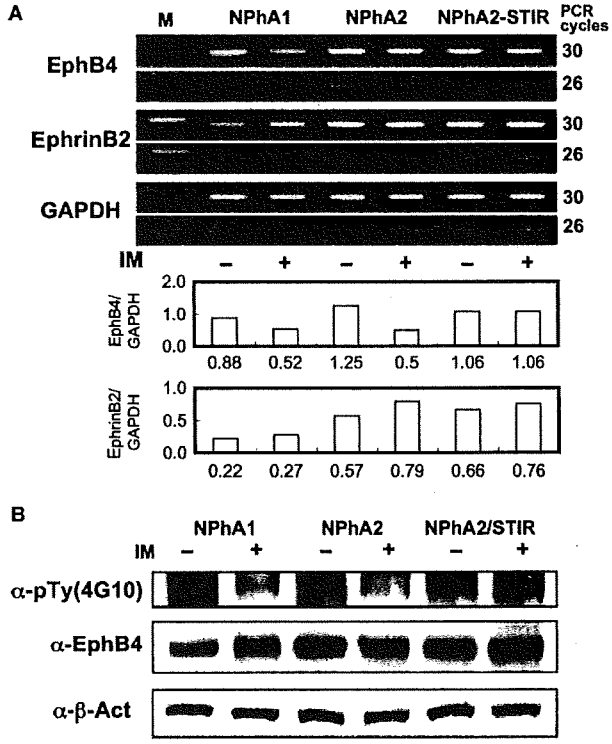

Figure 6 Expression of EphB4 and ephrinB2 and phosphorylation of EphB4. (A) Expression of *EphB4* and *ephrinB2* transcripts was compared by reverse transcription-PCR among NPhA1, NPhA2, and NPhA2/STIR cells before and after treatment with imatinib. Band intensity on gel electrophoresis was quantified using computer software as described in the text. (B) Expression and phosphorylation of EphB4 were analyzed by Western blotting. Whole-cell lysates were separated by SDS-PAGE, transferred to Hybond-C Extra membranes (GE Healthcare Bio-Sciences) and detected with the indicated antibodies.

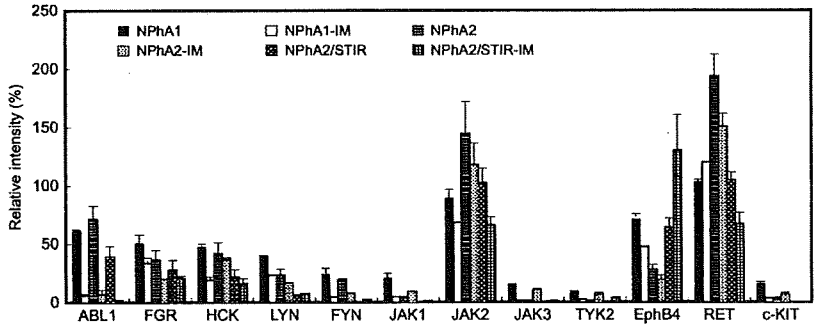

Figure 5 Phosphorylation antibody array analyses. Phosphorylated protein tyrosine kinases were detected using an antibody array. Imatinib-treated or untreated cell lysates were added to the antibody array membrane. Then, the membranes were washed and biotinylated anti-phosphotyrosine antibody was used to detect phosphorylated tyrosines on activated receptors. After incubation with HRP-conjugated streptavidin, array signals were visualized by chemiluminescent detection using X-ray film, and spot intensity was measured densitometrically.

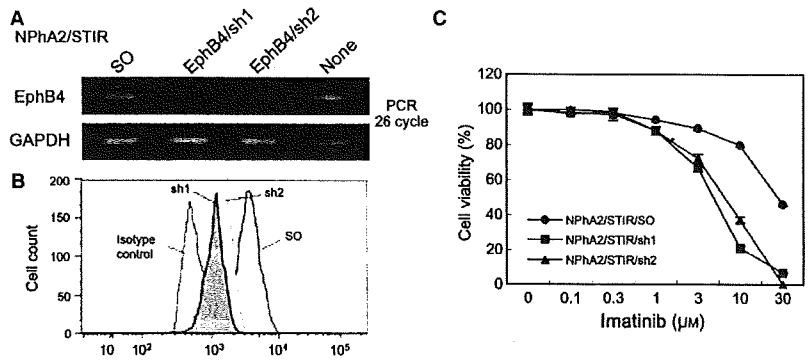

Figure 7 Analysis of EphB4 as a target of imatinib (IM) resistance. (A) Expression of *EphB4* transcript was inhibited with short hairpin (sh)RNA. We transduced the shRNAs sequence for *EphB4* or scramble oligonucleotide (SO) into NPhA2/STIR cells with a retroviral vector. Expression of *EphB4* transcript was analyzed by reverse transcription-PCR. (B) Surface expression of EphB4 was detected by FACS analysis. (C) Sensitivity of NPhA2/STIR/SO, NPhA2/STIR/sh1 and NPhA2/STIR/sh2 cells to IM. NPhA2/STIR/SO, NPhA2/STIR/sh1, and NPhA2/STIR/sh2 cells were added to 96-well plates with different concentrations of IM. Plates were incubated at 37°C for 96 h before addition of a mixture of tetrazolium and electron carrier. The cell proliferation assay was performed in triplicate, and mean absorption values are shown with their standard deviations. Three repeat experiments showed similar results.

Inhibition of EphB4 with shRNA

To analyze the role of EphB4 in IM resistance, EphB4 was knocked down with shRNA expressed by a retroviral vector. We tried two kinds of sh sequence, and established NPhA2/STIR/sh1 and NPhA2/STIR/sh2 cells in which the expression of *EphB4 RNA* was suppressed (Fig. 7A). FACS analysis showed that surface expression of EphB4 was reduced (Fig. 7B). The growth of NPhA2/STIR/sh1 and NPhA2/STIR/sh2 cells was inhibited by IM at concentrations above 3 μM; these cells were more sensitive than NPhA2/STIR but less sensitive than NPhA2 cells (Fig. 7C).

Discussion

We established cell lines derived from a patient with Ph^+ ALL and designated them NPhA1 (cells recovered at first diagnosis) and NPhA2 (cells recovered in the relapse phase). We also developed the IM-resistant cell line NPhA2/STIR from NPhA2 cells. NPhA2 cells showed mild IM resistance, and NPhA2/STIR proliferated in the presence of 10 μM IM, indicating strong IM resistance.

We examined the intracellular signaling pathway of these cell lines before and after IM treatment. NPhA2 cells acquired non-specific IM resistance in the relapse phase after conventional chemotherapy. Phosphorylation of LYN, HCK, EGR and JAK2, which were possible to be activated downstream of BCR-ABL (22, 23), was inhibited by IM, so that they were not likely to relate with IM-resistance in NPhA2 and NPhA2/STIR. Mild increases in MEK, ERK, and STAT3 phosphorylation and BCL-2 expression may be responsible for the mild IM resistance of NPhA2 cells. After IM treatment, NPhA2/STIR cells showed increased phosphorylation of MEK and ERK and a marked increase in RAS activation, which may play a role in BCR-ABL-independent strong IM resistance. Persistent activation of EphB4 after treatment with IM may be a partial contributor to the IM resistance of NPhA2/STIR cells.

The RAS signaling pathway plays an essential role in cancer cell growth. RAS activation leads to the phosphorylation and activation of downstream signaling proteins such as MEK and MAPK. Activation of the MAPK pathway was suggested as an explanation for the incomplete effect of IM on CML (24, 25). The RAS-independent activation of the MEK–MAPK pathway after IM administration was reported in pancreatic cancers, and addition of MEK inhibitor enhanced the inhibitory effect of IM on cancer cell growth (26). In our study, RAS was activated upstream of the MEK–MAPK pathway, but NRAS and KRAS mutations were not detected (data not shown). We obtained evidence that the induction of MEK–MAPK activation was induced after treatment with IM. IM may cancel negative feedback directed to the RAS–MAPK pathway or stimulate upstream RAS signaling. These results suggest a potential role for combined therapy with MEK inhibitor and IM in patients with BCR-ABL-independent IM resistance.

EphB4 is a member of the largest family of transmembrane receptor tyrosine kinases and has been shown to be related to the survival signal in several types of human malignant cells (27, 28), such as breast cancer, ovarian cancer, and squamous cell carcinoma cells. The significance of EphB4 and ephrinB2 coexpression in tumor advancement has also been described (29, 30). EphB4 is expressed in immature hematopoietic cells and its ligand ephrinB2 is expressed on BM stromal

cells and arterial endothelial cells (31). In this study, we screened 71 kinds of tyrosine kinase to determine their phosphorylation status using a tyrosine kinase antibody array and found that EphB4 was activated in Ph^+ cell lines. Activation of EphB4 was suppressed after IM treatment in NPhA1 and NPhA2 but not in NPhA2/STIR cells with increased expression of EphB4 and ephrinB2 transcripts. Although partial restoration of sensitivity to IM in NPhA2/STIR cells was observed after the introduction of EphB4 shRNA, the sensitivity of shRNA-containing NPhA2/STIR cells was not completely restored to the NPhA2 level. This may be a result of insufficient EphB4 suppression or the cumulative effects of other resistance mechanisms. The relationship between EphB4 and RAS activation remains to be elucidated in future studies.

We present here a new mechanism of IM resistance, i.e., the induction of RAS/MAPK activation, possibly related to EphB4. The results of this study also suggest a potential role of combined therapy with RAS/MAPK inhibitors and IM for Ph^+ ALL.

Acknowledgements

We thank Satoshi Suzuki and Chika Wakamatsu of Nagoya University for their skillful technical assistance. This study was supported by Grants-in-Aid from the Ministry of Education, Culture, Sports, Science and Technology, and the National Institute of Biomedical Innovation.

References

1. Druker BJ, Guilhot F, O'Brien SG, *et al.* Five-year follow-up of patients receiving imatinib for chronic myeloid leukemia. *N Engl J Med* 2006;**355**:2408–17.
2. O'Brien SG, Guilhot F, Larson RA, *et al.* Imatinib compared with interferon and low-dose cytarabine for newly diagnosed chronic-phase chronic myeloid leukemia. *N Engl J Med* 2003;**348**:994–1004.
3. Yanada M, Takeuchi J, Sugiura I, *et al.* High complete remission rate and promising outcome by combination of imatinib and chemotherapy for newly diagnosed BCR-ABL-positive acute lymphoblastic leukemia: a phase II study by the Japan Adult Leukemia Study Group. *J Clin Oncol* 2006;**24**:460–6.
4. Druker BJ, Sawyers CL, Kantarjian H, Resta DJ, Reese SF, Ford JM, Capdeville R, Talpaz M. Activity of a specific inhibitor of the BCR-ABL tyrosine kinase in the blast crisis of chronic myeloid leukemia and acute lymphoblastic leukemia with the Philadelphia chromosome. *N Engl J Med* 2001;**344**:1038–42.
5. Ottmann OG, Druker BJ, Sawyers CL, *et al.* A phase 2 study of imatinib in patients with relapsed or refractory Philadelphia chromosome-positive acute lymphoid leukemias. *Blood* 2002;**100**:1965–71.
6. Hofmann WK, Jones LC, Lemp NA, de Vos S, Gschaidmeier H, Hoelzer D, Ottmann OG, Koeffler HP. Ph(+) acute lymphoblastic leukemia resistant to the tyrosine kinase inhibitor STI571 has a unique BCR-ABL gene mutation. *Blood* 2002;**99**:1860–2.
7. Shah NP, Nicoll JM, Nagar B, Gorre ME, Paquette RL, Kuriyan J, Sawyers CL. Multiple BCR-ABL kinase domain mutations confer polyclonal resistance to the tyrosine kinase inhibitor imatinib (STI571) in chronic phase and blast crisis chronic myeloid leukemia. *Cancer Cell* 2002;**2**:117–25.
8. Redaelli S, Piazza R, Rostagno R, Magistroni V, Perini P, Marega M, Gambacorti-Passerini C, Boschelli F. Activity of bosutinib, dasatinib, and nilotinib against 18 imatinib-resistant BCR/ABL mutants. *J Clin Oncol* 2009;**27**:469–71.
9. le Coutre P, Tassi E, Varella-Garcia M, Barni R, Mologni L, Cabrita G, Marchesi E, Supino R, Gambacorti-Passerini C. Induction of resistance to the Abelson inhibitor STI571 in human leukemic cells through gene amplification. *Blood* 2000;**95**:1758–66.
10. Scappini B, Gatto S, Onida F, *et al.* Changes associated with the development of resistance to imatinib (STI571) in two leukemia cell lines expressing p210 Bcr/Abl protein. *Cancer* 2004;**100**:1459–71.
11. Mahon FX, Belloc F, Lagarde V, Chollet C, Moreau-Gaudry F, Reiffers J, Goldman JM, Melo JV. MDR1 gene overexpression confers resistance to imatinib mesylate in leukemia cell line models. *Blood* 2003;**101**:2368–73.
12. White DL, Saunders VA, Dang P, Engler J, Zannettino AC, Cambareri AC, Quinn SR, Manley PW, Hughes TP. OCT-1-mediated influx is a key determinant of the intracellular uptake of imatinib but not nilotinib (AMN107): reduced OCT-1 activity is the cause of low in vitro sensitivity to imatinib. *Blood* 2006;**108**:697–704.
13. Donato NJ, Wu JY, Stapley J, Gallick G, Lin H, Arlinghaus R, Talpaz M. BCR-ABL independence and LYN kinase overexpression in chronic myelogenous leukemia cells selected for resistance to STI571. *Blood* 2003;**101**:690–8.
14. Dai Y, Rahmani M, Corey SJ, Dent P, Grant S. A Bcr/Abl-independent, Lyn-dependent form of imatinib mesylate (STI-571) resistance is associated with altered expression of Bcl-2. *J Biol Chem* 2004;**279**:34227–39.
15. Abe A, Minami Y, Hayakawa F, *et al.* Retention but significant reduction of BCR-ABL transcript in hematopoietic stem cells in chronic myelogenous leukemia after imatinib therapy. *Int J Hematol* 2008;**88**:471–5.
16. Graham SM, Jorgensen HG, Allan E, Pearson C, Alcorn MJ, Richmond L, Holyoake TL. Primitive, quiescent, Philadelphia-positive stem cells from patients with chronic myeloid leukemia are insensitive to STI571 in vitro. *Blood* 2002;**99**:319–25.
17. Mishra S, Zhang B, Cunnick JM, Heisterkamp N, Groffen J. Resistance to imatinib of bcr/abl p190 lymphoblastic leukemia cells. *Cancer Res* 2006;**66**:5387–93.
18. Abe A, Kiyoi H, Ninomiya M, *et al.* Establishment of a stroma-dependent human acute myelomonocytic leukemia

cell line, NAMO-2, with FLT3 tandem duplication. *Int J Hematol* 2006;**84**:328–36.
19. Minami Y, Yamamoto K, Kiyoi H, Ueda R, Saito H, Naoe T. Different antiapoptotic pathways between wild-type and mutated FLT3: insights into therapeutic targets in leukemia. *Blood* 2003;**102**:2969–75.
20. Taylor SJ, Resnick RJ, Shalloway D. Nonradioactive determination of Ras-GTP levels using activated ras interaction assay. *Methods Enzymol* 2001;**333**:333–42.
21. Abe A, Emi N, Kanie T, Imagama S, Kuno Y, Takahashi M, Saito H, Naoe T. Expression cloning of oligomerization-activated genes with cell-proliferating potency by pseudotype retrovirus vector. *Biochem Biophys Res Commun* 2004;**320**:920–6.
22. Hu Y, Liu Y, Pelletier S, Buchdunger E, Warmuth M, Fabbro D, Hallek M, Van Etten RA, Li S. Requirement of Src kinases Lyn, Hck and Fgr for BCR-ABL1-induced B-lymphoblastic leukemia but not chronic myeloid leukemia. *Nat Genet* 2004;**36**:453–61.
23. Xie S, Wang Y, Liu J, Sun T, Wilson MB, Smithgall TE, Arlinghaus RB. Involvement of Jak2 tyrosine phosphorylation in Bcr-Abl transformation. *Oncogene* 2001;**20**:6188–95.
24. Agarwal A, Eide CA, Harlow A, Corbin AS, Mauro MJ, Druker BJ, Corless CL, Heinrich MC, Deininger MW. An activating KRAS mutation in imatinib-resistant chronic myeloid leukemia. *Leukemia* 2008;**22**:2269–72.
25. Chu S, Holtz M, Gupta M, Bhatia R. BCR/ABL kinase inhibition by imatinib mesylate enhances MAP kinase activity in chronic myelogenous leukemia CD34+ cells. *Blood* 2004;**103**:3167–74.
26. Takayama Y, Kokuryo T, Yokoyama Y, Nagino M, Nimura Y, Senga T, Hamaguchi M. MEK inhibitor enhances the inhibitory effect of imatinib on pancreatic cancer cell growth. *Cancer Lett* 2008;**264**:241–9.
27. Kumar SR, Singh J, Xia G, *et al.* Receptor tyrosine kinase EphB4 is a survival factor in breast cancer. *Am J Pathol* 2006;**169**:279–93.
28. Scehnet JS, Ley EJ, Krasnoperov V, Liu R, Manchanda PK, Sjoberg E, Kostecke AP, Gupta S, Kumar SR, Gill PS. The role of Ephs, Ephrins and growth factors in Kaposi sarcoma and implications of EphrinB2 blockade. *Blood* 2008;**113**:254–63.
29. Alam SM, Fujimoto J, Jahan I, Sato E, Tamaya T. Coexpression of EphB4 and ephrinB2 in tumour advancement of ovarian cancers. *Br J Cancer* 2008;**98**:845–51.
30. Yavrouian EJ, Sinha UK, Rice DH, Salam MT, Gill PS, Masood R. The significance of EphB4 and EphrinB2 expression and survival in head and neck squamous cell carcinoma. *Arch Otolaryngol Head Neck Surg* 2008;**134**:985–91.
31. Suenobu S, Takakura N, Inada T, Yamada Y, Yuasa H, Zhang XQ, Sakano S, Oike Y, Suda T. A role of EphB4 receptor and its ligand, ephrin-B2, in erythropoiesis. *Biochem Biophys Res Commun* 2002;**293**:1124–31.

Bone Marrow Transplantation (2010) 45, 363–369

www.nature.com/bmt

ORIGINAL ARTICLE

Donor single nucleotide polymorphism in the *CCR9* gene affects the incidence of skin GVHD

Y Inamoto[1,2], M Murata[1], A Katsumi[1], Y Kuwatsuka[2], A Tsujimura[2], Y Ishikawa[1], K Sugimoto[1], M Onizuka[2], S Terakura[1], T Nishida[2], T Kanie[2], H Taji[2], H Iida[2], R Suzuki[2], A Abe[1], H Kiyoi[3], T Matsushita[1], K Miyamura[2], Y Kodera[2] and T Naoe[1]

[1]*Department of Hematology and Oncology, Nagoya University Graduate School of Medicine, Nagoya, Japan;* [2]*Department of Hematology, Japanese Red Cross Nagoya First Hospital, Nagoya, Japan and* [3]*Department of Infectious Diseases, Nagoya University Graduate School of Medicine, Nagoya, Japan*

The interactions between chemokines and their receptors may have an important role in initiating GVHD after allogeneic hematopoietic SCT (allo-HSCT). CCL25 and CCR9 are unique because they are exclusively expressed in epithelial cells and in Peyer's patches of the small intestine. We focused on rs12721497 (G926A), one of the non-synonymous single nucleotide polymorphisms (SNPs) in the *CCR9* gene, and analyzed the SNP of donors in 167 consecutive patients who received allo-HSCT from an HLA-identical sibling donor. Genotypes were tested for associations with acute and chronic GVHD in each organ and transplant outcome. Multivariate analyses showed that the genotype 926AG was significantly associated with the incidence of acute stage ⩾2 skin GVHD (hazard ratio: 3.2; 95% confidence interval (95% CI): 1.1–9.1; $P=0.032$) and chronic skin GVHD (hazard ratio: 4.1; 95% CI: 1.1–15; $P=0.036$), but not with GVHD in other organs or with relapse, non-relapse mortality or OS. To clarify the functional differences between genotypes, each SNP in retroviral vectors was transfected into Jurkat cells. In chemotaxis assays, the 926G transfectant showed greater response to CCL25 than the 926A transfectant. In conclusion, more active homing of *CCR9*-926AG T cells to Peyer's patches may produce changes in Ag presentation and result in increased incidence of skin GVHD.
Bone Marrow Transplantation (2010) **45,** 363–369; doi:10.1038/bmt.2009.131; published online 15 June 2009
Keywords: allogeneic transplantation; CCR9; chemokine; gene polymorphism; GVHD

Correspondence: Dr A Katsumi, Department of Hematology and Oncology, Nagoya University Graduate School of Medicine, 65 Tsurumai-cho, Showa-ku, Nagoya 466-8560, Japan.
E-mail: katsumi@med.nagoya-u.ac.jp
Received 3 February 2009; revised 22 April 2009; accepted 24 April 2009; published online 15 June 2009

Introduction

Acute GVHD is a severe complication of allogeneic hematopoietic SCT (allo-HSCT).[1] After Ag presentation in secondary lymphoid tissues, migration of activated donor T lymphocytes to target organs has a central role in its induction. Recent studies have shown that the migration of lymphocytes to secondary lymphoid tissues or target organs, such as the skin, liver and gut, is regulated by specific chemokines.[2,3] Chemokines are a group of small molecules that regulate the trafficking of leukocytes through interactions with a subset of seven transmembrane, G protein-coupled receptors (chemokine receptors).[4,5] Their interactions may have an important role in initiating organ-specific GVHD.

Sites of expression are ubiquitous in many chemokines. For example, CCL17, which is well known as a skin-homing chemokine, is also expressed in many other organs, including the adrenal gland, bronchus, cerebellum, colon, heart and liver.[4] CCL28 is expressed by epithelial cells in several mucosal tissues, including the trachea, small intestine, colon, rectum, salivary gland and mammary gland.[6,7] By contrast, CCL25 (thymus-expressed chemokine) and its receptor CCR9 are unique because, outside the thymus, they are almost exclusively expressed by epithelial cells and Peyer's patches in the small intestine.[8–10] Therefore, we focused on CCR9 because it may influence the onset of intestinal GVHD or Ag presentation in Peyer's patches.

The *CCR9* gene is located on chromosome 3p21.3. A variety of single nucleotide polymorphisms (SNPs) in the *CCR9* gene have been reported, although their functional differences are not yet known. Within these SNPs, rs12721497 (G926A) is non-synonymous in exons, and it is the sole SNP whose frequency and linkage disequilibrium have been reported. This SNP alters the CCR9 amino acid sequence of the third exoloop from Val272 to Met272. We hypothesize that this SNP may have an effect on the onset of GVHD and transplant outcome because of the differences in the tissue-specific migration of T lymphocytes.

Materials and methods

Patients

A total of 186 consecutive patients received allogeneic BM or PBSC transplantation from an HLA-identical sibling donor at the Nagoya University Hospital and the Japanese Red Cross Nagoya First Hospital between 1987 and 2006. HLA matching among donor–recipient pairs was confirmed by either family study or genotyping in all patients. Of these 186 patients, 167 who received T-cell-replete transplantation and CYA in combination with short-term MTX as a GVHD prophylaxis were selected to participate in the study. CYA was administered daily at 3.0 mg/kg from day 1 as an i.v. infusion, and then switched to an oral dose at twice the i.v. dose when oral intake resumed. MTX was administered at 10 mg/m^2 on day 1 and, on days 3 and 6, was administered at 7 mg/m^2. Informed consent was obtained from all patients and donors, and the study was approved by the ethics committees at the Nagoya University Hospital and Japanese Red Cross Nagoya First Hospital.

Allellic discrimination of the polymorphism G926A in the CCR9 gene

The *CCR9*-G926A polymorphism (rs12721497) was determined by the PCR-RFLP method using genomic DNA obtained from donor PBMCs. The primers used for PCR were 5′-CACACCCTGATACAAGCCAA (forward) and 5′-CTCCAGCAACATAGACGACA (reverse). Sequences of interest were amplified by PCR, using Advantage II Polymerase Mix (Clontech Laboratories, Mountain View, CA, USA) in reaction mixtures containing 0.5 μl of genomic DNA and 10 pmol of each primer in a volume of 20 μl. Amplifications were performed using 35 cycles of denaturation at 95 °C for 30 s, annealing at 65 °C for 15 s and elongation at 72 °C for 30 s on a model 9600 thermocycler (Perkin-Elmer, Norwalk, CT, USA). After amplification, the 369-bp *CCR9* fragment was digested for 2 h at 37 °C with 5 U of *NLA*III (New England BioLabs, Ipswich, MA, USA) in a 20 μl reaction mixture. The digested products were analyzed by electrophoresis on a 1.5% agarose gel. Wild-type (AA) individuals were identified by the presence of only a 369-bp fragment, heterozygotes (AG) by the presence of both 231/138- and 369-bp fragments and homozygotes (GG) by the presence of only the 231- and 138-bp fragments. To rule out the incomplete digestion of the AG genotype, PCR products of this genotype were directly sequenced using the Applied Biosystems 310 automated DNA sequencer (Applied Biosystems, Foster City, CA, USA) following the manufacturer's instructions.

Site-directed mutagenesis and construction of CCR9-926A and 926G expression vectors

Site-directed mutagenesis of the human wild-type *CCR9* cDNA in pF1K vector (purchased from Kazusa DNA Research Institute, Kisarazu, Chiba, Japan) was carried out using the Quickchange Kit (Stratagene, La Jolla, CA, USA). Synthetic oligonucleotide primers containing the corresponding 926G point mutation had the following sequences: 5′-CCATTGACGCCTATGCCGTGTTCATC TCCAACTGT (forward) and 5′-ACAGTTGGAGA TGAACACGGCATAGGCGTCAATGG (reverse). The oligonucleotide was amplified with Pfu turbo DNA polymerase (Stratagene), and the template plasmid was digested by *Dpn*I. Each sequence of *CCR9* cDNA was amplified by PCR with primers containing the following *Eco*RI/*Not*I sites: 5′-CGCGGAATTCATGACACCCAC AGACTTCACA (forward) and 5′-ATCGGCGGCCGC TCAGAGGGAGAGTGCTCCTGAGGT (reverse). Each product was cut at *Eco*RI/*Not*I sites, and ligated into pMX-IRES-Puro (a kind gift from Dr Toshio Kitamura, University of Tokyo), which had been digested with *Eco*RI and *Not*I. The final construct used for cell transfection was sequenced entirely to verify the presence of the mutation and to ensure that no other variant was accidentally introduced during DNA amplification.

Retrovirus transfection

PLAT-A packaging cells (a kind gift from Dr Toshio Kitamura, University of Tokyo) were used to produce recombinant retrovirus particles.[11] PLAT-A cells were transfected with retroviral vectors using FuGENE6 (Roche, Indianapolis, MN, USA). Jurkat cells were infected with each of the pMX-CCR9-926A-IRES-Puro, pMX-CCR9-926G-IRES-Puro and pMX-IRES-Puro (control) retroviruses. The cells were washed once and resuspended in the fresh selection medium containing 500 ng/ml of puromycin (Cayla, Toulouse, France), 48 h after transfection .

Flow cytometric analysis

Phycoerythrin-labeled monoclonal anti-CCR9 (112509) was purchased from R&D Systems (Minneapolis, MN, USA). Analyses were carried out on FACSAria (BD Biosciences, San Jose, CA, USA) using the FlowJo software (Treestar, San Carlos, CA, USA).

Chemotaxis assays

Chemotaxis assays were carried out as previously described[12] using 6.5-mm-thick Transwell tissue culture inserts with a 5-μm pore size (Corning, Corning, NY, USA). The transfected cell lines were starved overnight in the plain RPMI 1640 medium, suspended at 1×10^7 cells per ml in this medium with 0.1% of BSA, and 100 μl of cell suspension was added to an upper insert in a lower well with 600 μl of the medium. After equilibration at 37 °C for 2 h, various concentrations (0–2000 ng/ml) of recombinant human CCL25 (R&D Systems) were added to the lower wells, and the plates were incubated for an additional 90 min before migrated cells in the lower well were counted.

Statistical analysis

OS was calculated from the date of transplantation to the date of death from any cause using the Kaplan–Meier method, and *P*-values were calculated using a log-rank test. Non-relapse mortality (NRM) was defined as mortality due to any cause other than relapse or disease progression. Cumulative incidences of NRM and relapse were estimated